OXYGEN DISTRIBUTION AND MIGRATION WITHIN $Mb^{des\ Fe}$ AND $Hb^{des\ Fe}$

Multifrequency Phase and Modulation Fluorometry Study

DAVID M. JAMESON, ENRICO GRATTON, AND GREGORIO WEBER
Departments of Biochemistry and Physics, University of Illinois at Urbana-Champaign, Urbana, Illinois 61801

BERNARD ALPERT
Laboratoire de Biologie-Chimique, Université de Paris VII, Paris, France

ABSTRACT Quenching of the intensity and lifetime of porphyrin fluorescence from $Mb^{des\ Fe}$ and $Hb^{des\ Fe}$ (iron-free myoglobin and hemoglobin) by oxygen was investigated using a multifrequency cross-correlation phase fluorometer. The single exponential decay characteristic of porphyrin emission of $Mb^{des\ Fe}$ and $Hb^{des\ Fe}$ became doubly exponential upon application of oxygen pressure. The results were interpreted in terms of a general model of dynamic quenching of fluorescence in globular proteins. The model accounted for the rate k^+ of acquisition of quencher by the protein, the exit rate k^- of quencher from the protein, and the migration rate χ of quencher in the protein interior. The values of k^+, k^-, and χ were different for $Mb^{des\ Fe}$ and $Hb^{des\ Fe}$. The addition of 40% sucrose, which increased the bulk viscosity sixfold, modified these rates. These results are discussed and compared with previous quenching studies on proteins. The significance of these results and the model for the interpretation of protein quenching studies is emphasized.

INTRODUCTION

During the past decade fluorescence quenching experiments have contributed substantially to our understanding of internal dynamics of proteins (see reference 1 for a recent review of the literature in this area). The information available from such studies has generally been limited to a characterization of the quenching process in terms of static and dynamic contributions; many details of this process still remain obscure. The additional information required includes the partition coefficient for the quencher between the protein and solvent phases, the rate of acquisition of the quencher by the protein, a description of the migration of the quencher in the protein interior, and the details of the distribution of quenchers throughout the protein ensemble. Additional useful information can be derived from the effect of solvent viscosity upon the migration of quencher in the protein interior.

In an effort to obtain this information, we have studied the quenching by molecular oxygen of the porphyrin emission of $Mb^{des\ Fe}$ and $Hb^{des\ Fe}$, the iron-free derivatives of myoglobin and hemoglobin, respectively (note that the absence of iron precludes the binding of oxygen to the heme moiety). The choice of oxygen is suggested by the well-established fact that oxygen is a nonpolar, unity quencher that diffuses readily within the protein interior (2). The choice of $Mb^{des\ Fe}$ and $Hb^{des\ Fe}$ as protein systems and oxygen as quencher is justified considering both the intrinsic importance of these proteins as oxygen carriers in biological systems as well as the wealth of structural information available. Furthermore, the relatively long lifetime of the porphyrin fluorescence turned out to be an essential feature for the interpretation of the results as discussed in the preceeding article where the theory of the quenching process in globular proteins was developed. The effect of solvent viscosity upon quenching was studied by the addition of sucrose (40% wt/wt) to the protein solutions, which increased the bulk viscosity by a factor of 6 (3).

MATERIALS AND METHODS

$Mb^{des\ Fe}$ and $Hb^{des\ Fe}$ were prepared from horse myoglobin (Sigma Chemical Co., St. Louis, MO) and human hemoglobin, respectively. The refolding of the apoglobins after the heme extraction was carried out in 0.01 M bis-Tris buffer, pH 6.0. The association of the globins with protoporphyrin IX (Sigma Chemical Co.) was done according to previously published procedures (4). The final step in the purification of $Mb^{des\ Fe}$ differed from that of $Hb^{des\ Fe}$, though. In lieu of the CMC-52 chromatographic step $Mb^{des\ Fe}$ was dialyzed for 12 h at 4°C against distilled water (1 volume sample for 100 volumes water) and then passed through a mixed-bed resin (model No. AG 501, Bio-Rad Laboratories, Richmond, CA). These procedures removed the excess porphyrin as well as any aberrent porphyrin-protein adducts. The quality of the final

Dr. Jameson's present address is the Department of Pharmacology, University of Texas Health Science Center at Dallas, Dallas, TX 75235

products was investigated with several techniques including chromatography, ultracentrifugation and absorption and emission spectroscopy.

All quenching experiments were done in 10 mM potassium phosphate buffer, pH 7.0, at 20°C ± 0.2°C with protein concentrations near 5×10^{-6} M. At this concentration, the $Mb^{des\ Fe}$ and $Hb^{des\ Fe}$ exist in the momomeric and tetrameric forms, respectively, as shown by sedimentation coefficients and fluorescence polarization data. Oxygen quenching was performed using a pressure cell similar to that described by Lakowicz and Weber (5); solutions were maintained in a quartz fluorescence cuvette that was 2 cm on each side. Pressure of the gas over the solutions were determined with a Roylyn precision gauge (0–1,500 psi [pounds per square inch] scale) (Roylyn Rueher Precision, Santa Ana, CA.). The sample was stirred continuously with a magnetic stirrer that achieved equilibration between gas and solution phases in <1 h. The sample was illuminated only during the fluorescence measurement period that lasted a few minutes at each oxygen pressure. No alterations in the visible region of the absorption spectra of $Mb^{des\ Fe}$ and $Hb^{des\ Fe}$ were evident under 1,500 psi of oxygen; similar results were obtained for deoxyhemoglobin under 1,500 psi of nitrogen and oxyhemoglobin under 1,500 psi of oxygen. The solubility of oxygen in water and in a 40% aqueous sucrose solution at 20°C is 9.38×10^{-5} M/psi and 6×10^{-5} M/psi, respectively (6). The sucrose (Schwarz/Mann, Orangeburg, NY) was twice recrystallized from an ethanol-water solution. The visible absorption spectra and the porphyrin emission spectra of $Mb^{des\ Fe}$ and $Hb^{des\ Fe}$ were not altered by sucrose addition. Also, addition of 40% sucrose to a hemoglobin solution did not alter the cooperative aspect of the oxygen binding, nor was the magnitude of the Bohr effect altered. The absence of energy transfer among the porphyrin moieties of the different subunits of $Hb^{des\ Fe}$ was demonstrated by polarization data. Specifically, Perrin plots for the porphyrin polarization at various excitation wavelengths yielded P_o (limiting polarization) values identical to those obtained for dilute solutions of protoporphyrin IX in propylene glycol at −55°C (7).

Fluorescence lifetime measurements were performed with a multifrequency cross-correlation phase fluorometer, the operational details of which have been reported (8). The measured quantities, τ^P and τ^M, represent the lifetimes measured by phase delay and demodulation of the emission relative to a scattering signal. For the experiments described in this report the laser was tuned at 501 nm. The modulation frequencies chosen were 6, 12, 18, 24, 30, and 36 MHz. The porphyrin emission was observed through a 1/4-meter grating nomochromator (Jarell Ash, Div. Fisher Scientific Co., Waltham, MA) set at 630 nm with a bandwidth of 3 nm. A Corning 2-64 (Corning Medical and Scientific Medfield, MA) filter was interposed between the sample and the monochromator to further reject scattered light and the plasma discharge from the laser tube. The reference signal for the phase and modulation measurements was derived from scattered light observed through the monochromator set at the illuminating wavelength (with the filter removed). A stable, accurate reference signal could be obtained from the intrinsic Rayleigh scatter of the sample solution, which rendered addition of foreign scattering materials such as glycogen unnecessary. The fluorescence intensity was measured on the same apparatus for each value of the oxygen pressure. The laser was operated in the light control mode, and the average excitation intensity, measured by a reference photomultiplier, remained constant for the duration of the experiment. The light intensity utilized did not lead to photobleaching effects in this system. Slow removal of the oxygen resulted in complete recovery of the initial lifetime values.

RESULTS

The experimental data for $Mb^{des\ Fe}$ and $Hb^{des\ Fe}$ consists of a set of lifetimes, τ^P and τ^M, at six modulation frequencies, and fluorescence intensities as a function of the oxygen pressure. These results for $Hb^{des\ Fe}$ and $Mb^{des\ Fe}$ for 12 MHz and 30 MHz modulation are shown in Table I, while Fig. 1 shows the traditional mode of presentation for such data for $Hb^{des\ Fe}$. A common feature of the data for each protein in the absence of oxygen was that the lifetimes measured by phase (τ^P) and modulation (τ^M) were identical at all modulation frequencies, indicating a homogeneous emitting population (9). As the oxygen pressure increased, the lifetimes determined by phase and modulation became different and dependent upon the modulation frequency, indicating a heterogeneous emitting population. The data were analyzed according to the model described in the preceding article (10). The phase and modulation data were fit using a nonlinear least-squares routine described elsewhere (11).

TABLE I
PHASE AND MODULATION LIFETIMES AND RELATIVE INTENSITIES AS A FUNCTION OF OXYGEN PRESSURE FOR $Mb^{des\ Fe}$ AND $Hb^{des\ Fe}$

Protein	Pressure	12 MHz		30 MHz		Intensity normalized)
		τ^P	τ^M	τ^P	τ^M	
	psi	*ns*	*ns*	*ns*	*ns*	
$Mb^{des\ Fe}$	3	18.74	18.42	18.40	18.47	1.000
	310	15.02	15.10	15.12	14.94	0.658
	610	12.58	12.87	12.08	12.52	0.483
	905	10.96	11.45	10.09	11.14	0.340
	1,205	9.64	10.00	8.80	9.71	0.267
	1,510	8.57	9.00	7.66	8.61	0.207
$Hb^{des\ Fe}$	3	20.11	20.06	20.30	20.41	1.000
	275	12.94	14.64	10.30	13.83	0.461
	515	10.10	11.75	7.88	10.75	0.305
	745	8.27	10.02	6.42	9.09	0.206
	990	7.03	8.81	5.49	7.86	0.172
	1,250	6.05	7.75	4.82	6.82	0.141

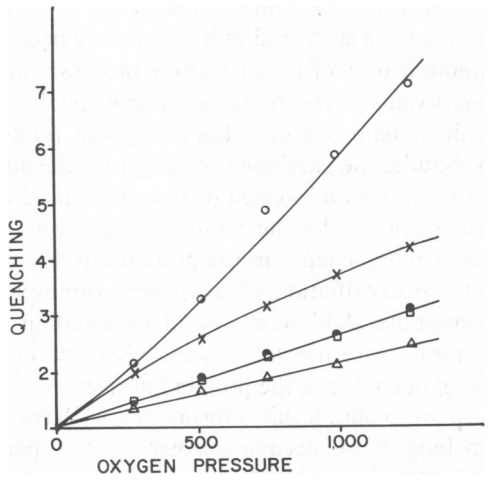

FIGURE 1 Oxygen quenching of the intensity and lifetime of porphyrin emission from $Hb^{des\ Fe}$. O, F_0/F; ×, τ_0/τ^P (at 30 MHz); ●, τ_0/τ_M (at 30 MHz); □, τ_0/τ^P (at 12 MHz); Δ, τ_0/τ^M (at 12 MHz) where F_o and F are the intensities in the absence and presence of quencher, τ_o is the lifetime in the absence of quencher, and τ^P and τ^M are the phase and modulation lifetimes in the presence of quencher. Oxygen pressure is given in pounds per square inch.

The equations for the model proposed in the preceding article were derived for the case of pulse excitation, while the experiments described in this report were performed using a phase and modulation fluorometer. The corresponding equations for sinusoidal excitation can be derived from the following considerations. The impulse response of the system is described by a sum of exponentially decaying components (Eq. 7 of reference 10):

$$F(t) = \sum_i \alpha_i e^{-m_i t} \tag{1}$$

where α_i is the amplitude and m_i the characteristic decay rate for each component. The sine and cosine transforms of the impulse response (9) are given by

$$S(\omega) = \int_0^\infty F(t) \sin(\omega t) \mathrm{d}\, t \tag{2}$$

$$G(\omega) = \int_0^\infty F(t) \cos(\omega t) \mathrm{d}\, t \tag{3}$$

where ω ($= 2\pi f$) is the angular modulation frequency.

The general expressions for the $S(\omega)$ and $G(\omega)$ functions are then (9)

$$S(\omega) = \sum_i f_i\, \omega/(\omega^2 + m_i^2) \tag{4}$$

$$G(\omega) = \sum_i f_i m_i/(\omega^2 + m_i^2) \tag{5}$$

where f_i is the fractional intensity of each component defined by

$$f_i = (\alpha_i/m_i)/(\sum_j \alpha_j/m_j) \tag{6}$$

where the index j runs over all components.

For each value of the frequency one may calculate a value for the modulation ratio and phase delay in terms of the functions $S(\omega)$ and $G(\omega)$:

$$\phi = \tan^{-1}\,[S(\omega)/G(\omega)] \tag{7}$$

$$M = [S(\omega^2) + G(\omega^2)]^{1/2}. \tag{8}$$

The function minimized by the least-squares routine was

$$LS = \sum_i [(\phi_i^{ex} - \phi_i^c)/\sigma_i^\phi]^2 + \sum [(m_i^{ex} - m_i^c)/\sigma_i^m]^2 \tag{9}$$

where σ_i^ϕ and σ_i^m are the standard deviations associated with each measurement (11). The superscripts ex and c indicate measured and calculated values, respectively, We compared the quality of the fit of experimental data to the theoretical curve using the expression

$$SQM = (LS)^{1/2}/N \tag{10}$$

where N is the number of measurements for each set of data. The computer program fits for two exponential components (11, 12). Three parameters were obtained (Table II): two lifetime values (τ_0 and τ_1) and one fractional component (f_0). We observe that the quality of the fit is very good for the entire set of data as judged from the low value of *SQM* (a good fit gives values of *SQM* <0.1). In Figs. 2 and 3 we report the phase and modulation data and least-squares analysis for $Hb^{des\ Fe}$ in the absence and presence of oxygen, respectively. The values of $m_0(=1/\tau_0)$, $m_1(=1/\tau_1)$ and f_0 for $Mb^{des\ Fe}$ and $Hb^{des\ Fe}$, in the presence and absence of sucrose, are shown in Figs. 4–9. Four parameters k^+, k^-, χ, and Γ were obtained using the procedure described in the preceding article. These parameters correspond to the rate of acquisition of quencher by the protein (k^+), the exit rate of quencher from the protein (k^-), the migration rate of quencher in the protein interior (χ), and the radiative decay rate of the fluorophore (Γ). The initial slope of the plot of m_0 vs. oxygen concentration equals k^+, whereas the intercept equals Γ. These values of $Mb^{des\ Fe}$ and $Hb^{des\ Fe}$ in the presence and absence of sucrose are reported in Table III. As predicted by the model, the rate m_1 was independent of

TABLE II

RESULTS OF LEAST-SQUARES ANALYSIS FOR $Mb^{des\ Fe}$ AND $Hb^{des\ Fe}$ IN PRESENCE AND ABSENCE OF SUCROSE

Pressure	τ_0	f_0	τ_1	*SOM*
PSI	*ns*		*ns*	
$Mb^{des\ Fe}$				
3	17.88 ± 0.13	1.04 ± 0.01	6.34 ± 0.74	0.040
310	15.21 ± 0.07	1.00 ± 0.01	2.65 ± 3.86	0.052
610	13.08 ± 0.06	0.97 ± 0.01	3.92 ± 0.51	0.034
905	11.65 ± 0.05	0.95 ± 0.01	3.18 ± 0.26	0.030
1205	10.47 ± 0.07	0.92 ± 0.01	2.92 ± 0.26	0.037
1510	9.73 ± 0.09	0.87 ± 0.01	3.24 ± 0.21	0.040
$Mb^{des\ Fe}$ (40% sucrose)				
3	18.45 ± 0.21	0.99 ± 0.03	10.94 ± 6.17	0.021
310	17.08 ± 0.08	0.97 ± 0.01	5.89 ± 0.55	0.029
610	15.49 ± 0.08	0.96 ± 0.01	4.11 ± 0.38	0.042
905	13.93 ± 0.08	0.94 ± 0.01	3.55 ± 0.30	0.048
1250	13.00 ± 0.11	0.92 ± 0.01	3.51 ± 0.30	0.060
1510	12.27 ± 0.18	0.90 ± 0.01	3.23 ± 0.26	0.065
$Hb^{des\ Fe}$				
3	20.65 ± 0.08	0.99 ± 0.01	2.34 ± 0.01	0.055
275	14.54 ± 0.09	0.95 ± 0.01	0.20 ± 0.71	0.093
515	12.10 ± 0.08	0.88 ± 0.01	1.83 ± 0.15	0.061
745	10.09 ± 0.07	0.86 ± 0.01	1.01 ± 0.12	0.058
990	9.51 ± 0.12	0.75 ± 0.01	2.10 ± 0.09	0.065
1250	8.37 ± 0.10	0.72 ± 0.01	1.83 ± 0.12	0.065
$Hb^{des\ Fe}$				
3	20.28 ± 0.03	1.00 ± 0.01	0.15 ± 2.68	0.038
320	17.86 ± 0.10	0.90 ± 0.01	5.98 ± 0.19	0.038
615	15.44 ± 0.10	0.82 ± 0.01	4.57 ± 0.09	0.042
915	13.81 ± 0.15	0.74 ± 0.01	4.08 ± 0.09	0.059
1205	12.53 ± 0.20	0.68 ± 0.01	3.67 ± 0.01	0.073

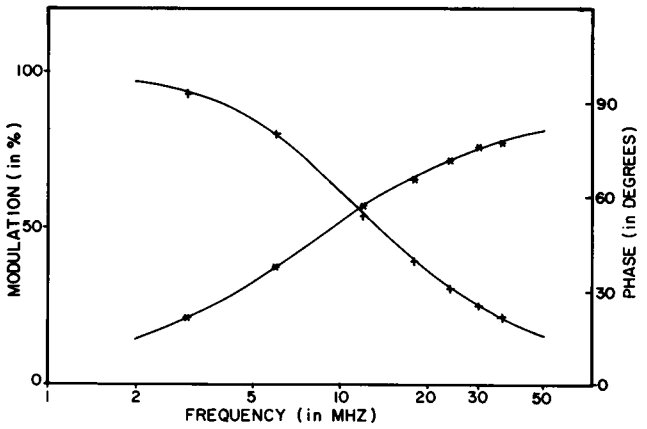

FIGURE 2 Multifrequency phase (*) and modulation (+) values for $Hb^{des\ Fe}$ at 3 psi of oxygen. Solid lines (—) indicate the fit to a single exponential decay of 20.18 ns.

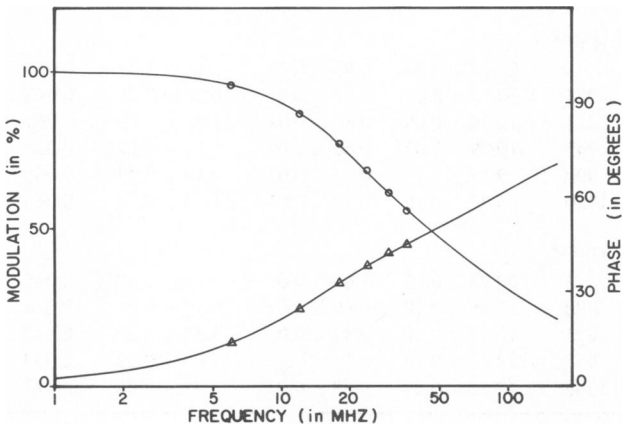

FIGURE 3 Multifrequency phase (Δ) and modulation (o) values for $Hb^{des\ Fe}$ at 1,250 psi of oxygen. Solid lines (—) indicate the fit for two exponential components $\tau_0 = 8.37$ ns, and $\tau = 1.83$ ns, and $f_0 = 0.72$.

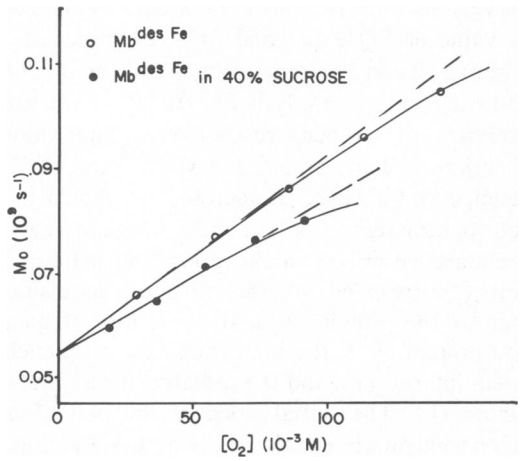

FIGURE 4 A plot of m_0 vs. oxygen concentration for $Mb^{des\ Fe}$ in the absence (o) and presence (•) of sucrose. Broken lines (---) correspond to the initial slopes.

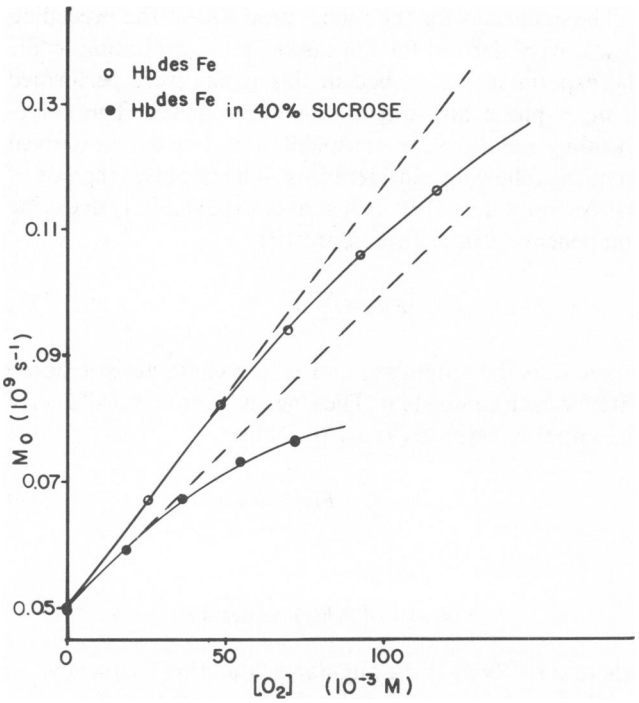

FIGURE 5 A plot of m_0 vs. oxygen concentration for $Hb^{des\ Fe}$ in the absence (o) and presence (•) of sucrose. Broken lines (---) correspond to the initial slopes.

the oxygen pressure in the limit of low oxygen concentration. Extrapolation to zero oxygen concentration was difficult, though. The error on m_1 increased at low oxygen pressure, since the fractional weight of this short component decreases with the oxygen concentration. To circumvent this difficulty, the weighted average of the m_1 values were used to calculate an alternative fit of the experimental data (broken lines in Figs. 6 and 7). The results of these fits are reported in Table IV. The new fits still appear very good judging by the low values of the *SQM*'s, justifying the choices of m_1.

The value of m_1 depends on the sum of χ and k^-. To

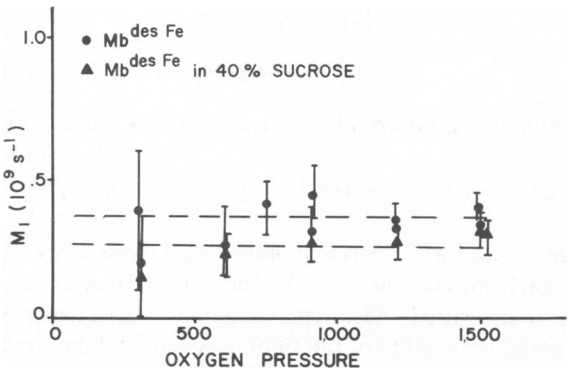

FIGURE 6 A plot of m_1 vs. oxygen pressure for $Mb^{des\ Fe}$ in the absence (•) and presence (Δ) of sucrose. Broken lines (---) indicate the approximate average values of $0.36 \times 10^9\ s^{-1}$ and $0.26 \times 10^9\ s^{-1}$ in the absence and presence of sucrose, respectively.

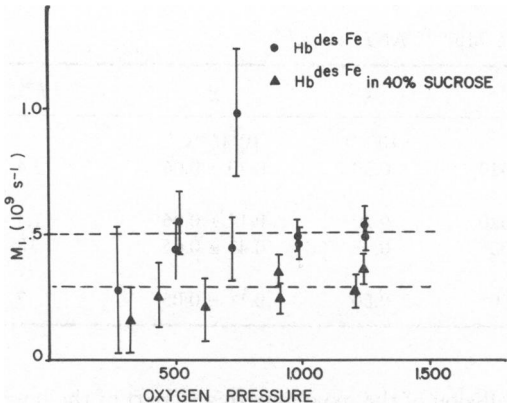

FIGURE 7 A plot of m_1 vs. oxygen pressure for $Hb^{des\ Fe}$ in the absence (●) and presence (Δ) of sucrose. Broken lines (---) indicate the approximate average values of $0.5 \times 10^9\ s^{-1}$ and $0.25 \times 10^9\ s^{-1}$ in the absence and presence of sucrose, respectively.

calculate χ and k^- separately f_o, the fraction of the component of lifetime τ_o, must be analyzed as a function of the oxygen pressure. As shown in the preceeding article, the initial slope of the f_o vs. oxygen pressure can be used to calculate k^-; these values are reported in Table III.

DISCUSSION

The interpretation of the complete quenching curves is complex, and, as discussed in the preceeding article (10), we distinguish here between two regimes, namely, the low and high quencher concentration regimes. We limit our initial discussion to the analysis of data from the low quencher concentration regime where consideration of the details of the quencher distribution in the protein ensemble is not important. We first consider the physical interpretation of the phenomological parameters, k^+, k^-, and χ. We must distinguish at the outset the different physical interpretation of these parameters for the case of fluorophore

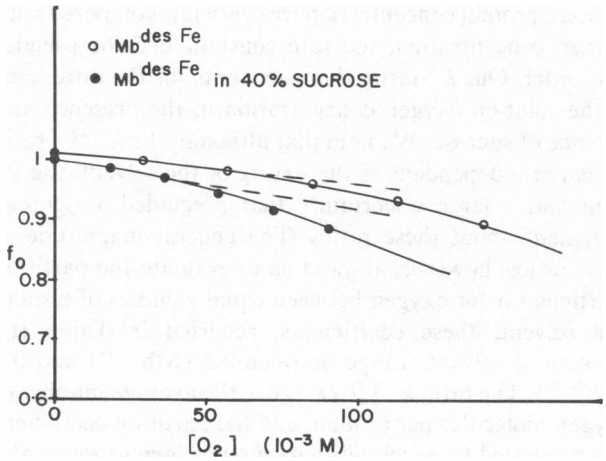

FIGURE 8 A plot of fractional intensity, f_o, vs. oxygen concentration for $Mb^{des\ Fe}$ in the absence (○) and presence (●) of sucrose.

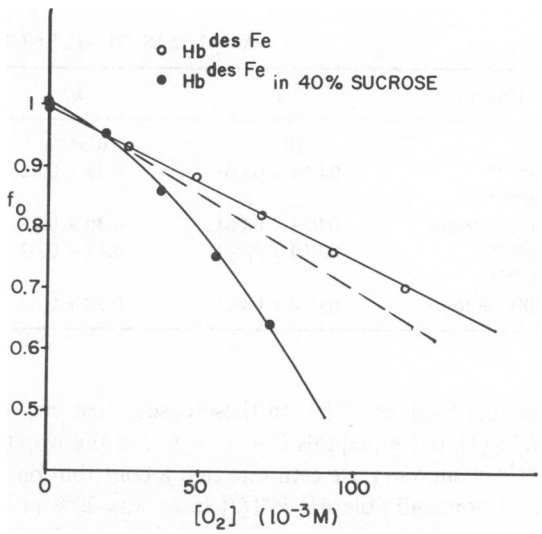

FIGURE 9 A plot of fractional intensity, f_o, vs. oxygen concentration for $Hb^{des\ Fe}$ in the absence (○) and presence (●) of sucrose.

free in solution and for the case of proteins, a distinction pointed out in the preceeding article.

For the case of free fluorophore in solution, k^+ corresponds to the rate of association between quencher and fluorophore. For the protein case we do not envision a well-defined quencher-protein complex , but rather we picture k^+ as the rate of acquisition of quencher by the protein; we shall not specify the microscopic details of this acquisition process. We note, however, that several microscopic processes may be important and may occur contemporaneously. The actual values obtained for k^+ in our experiments represent average values that will limit the possible microscopic scenerios.

Similar considerations apply for the k^- term that, in the case of free fluorophore, corresponds to the dissociation rate of the complex, but in the case of proteins corresponds to the exit rate of quencher from the protein. The term χ, in the case of free fluorophore, corresponds to the rate of deactivation of the excited state regardless of mechanism. In the case of a fluorophore buried in the protein interior, however, the quenching process requires the migration of the quencher through the protein matrix to the vicinity of the fluorophore. Our viewpoint is that this migration process requires rapid fluctuations in the protein matrix. The actual measured values of χ represent an average for the many possible migration processes that may be operating contemporaneously.

We comment now on the actual magnitudes of our measured parameters, k^+, k^-, and χ. The values for k^+, obtained from the initial slope of the m_0 vs. oxygen concentration plots, were determined with a relatively high precision (see Table III). We should, however, note the possibility of a small systematic contribution to k^+ due to the nature of the analysis. Specifically with regard to Eq. 6 of the preceeding article, we note that the term $4k^-k^+[Q]$ becomes negligible in the limit of low quencher concentra-

TABLE III
ANALYSIS OF QUENCHING DATA FOR $Mb^{des\ Fe}$ AND $Hb^{des\ Fe}$

Protein	Γ	k^+	k^-	α	χ	k^*_{app}
	$10^9 s^{-1}$	$10^9 M^{-1}s^{-1}$	$10^9 s^{-1}$	$10^9 s^{-1}$	$10^9 M^{-1}s^{-1}$	
$Mb^{des\ Fe}$	0.054 ± 0.001	0.38 ± 0.02	0.110 ± 0.020	0.30	0.20 ± 0.06	2.4
$Mb^{des\ Fe}$ (40% sucrose)	0.054 ± 0.001	0.30 ± 0.02	0.090 ± 0.020	0.30	0.12 ± 0.06	1.4
$Hb^{des\ Fe}$	0.050 ± 0.001	0.67 ± 0.02	0.026 ± 0.005	0.58	0.42 ± 0.05	18
$Hb^{des\ Fe}$ (40% sucrose)	0.050 ± 0.001	0.50 ± 0.02	0.022 ± 0.005	0.60	0.18 ± 0.05	7

tion or small values of k^-. In these cases, then, m_0 equals $\Gamma + k^+[Q]$ and m_1 equals $\Gamma + \chi + k^-$. In the worst case ($Mb^{des\ Fe}$ in sucrose), we estimate that a contribution to k^+ due to a nonnegligible $4k^-k^+[Q]$ term was 20% at most. The measured k^+ values, which ranged from 0.3 to 0.7 × 10^9 $M^{-1}s^{-1}$, were significantly lower than the diffusion-controlled quenching rate of porphyrin by oxygen in fluid solvents, which is ~1.1 × 10^{10} M^1 s^{-1} (13). Our k^+ values taken together with their small dependence upon solvent viscosity rule out a significant contribution to the quenching by oxygen in the solvent. These k^+ values were also approximately an order of magnitude larger than the rate constants observed for the binding of oxygen to myoglobin and hemoglobin (in the limit of the first oxygen bound). Because we did not measure binding in our experiments but simply a quenching process that presumably occurs upon collision of the oxygen with any part of the porphyrin moiety, our k^+ values should be higher than the binding constants. These k^+ values were in the range of those obtained for the quenching of pyrenebutyrate–bovine serum albumin adducts by oxygen (14) (a case discussed in the preceeding article), the quenching of the triplet absorption of $Mb^{des\ Fe}$ and $Hb^{des\ Fe}$ by oxygen (15) and the penetration rate for oxygen into myoglobin (in glycerol/water 3:1) determined by flash photolysis experiments at room temperatures (16).

TABLE IV
RESULTS OF LEAST-SQUARES ANALYSIS FOR $Mb^{des\ Fe}$ AND $Hb^{des\ Fe}$ IN PRESENCE AND ABSENCE OF SUCROSE WITH τ_1 FIXED

	M	τ_0	f_0	m_0	F_0/F	SQM
	mM/liter	ns		$10^9 s^{-1}$		
$Mb^{des\ Fe}$	0.2	18.31	1.01	0.055	0.93	0.063
(τ_1 = 2.8 ns)	29.1	15.21	0.99	0.066	1.22	0.052
	57.3	12.97	0.98	0.077	1.51	0.036
	85.0	11.59	0.96	0.086	1.79	0.031
	113.1	10.44	0.93	0.096	2.08	0.037
	141.7	9.56	0.89	0.105	2.41	0.040
$Mb^{des\ Fe}$	0.2	18.32	1.00	0.055	1.00	0.022
(40% sucrose)	18.6	16.88	0.99	0.059	1.14	0.030
(τ_1 = 3.8 ns)	54.3	13.99	0.94	0.071	1.51	0.049
	72.3	13.10	0.91	0.076	1.69	0.061
	90.6	12.50	0.88	0.080	1.85	0.070
$Hb^{des\ Fe}$	0.2	20.60	0.91	0.047	1.08	0.053
(τ_1 = 2.0 ns)	25.8	14.98	0.93	0.067	2.02	0.127
	48.3	12.19	0.88	0.082	2.75	0.062
	69.9	10.63	0.82	0.094	3.47	0.088
	92.9	9.39	0.76	0.106	4.15	0.065
	117.3	8.56	0.70	0.116	4.78	0.067
$Hb^{des\ Fe}$	0.2	20.04	1.01	0.050	0.94	0.066
(40% sucrose)	19.2	17.04	0.95	0.059	1.36	0.078
(τ_1 = 4.8 ns)	36.9	14.92	0.86	0.067	1.87	0.059
	54.9	13.66	0.75	0.073	2.34	0.059
	72.3	13.16	0.64	0.076	2.79	0.087

The values of k^- (and χ) have larger uncertainties than the k^+ values, since m_1 was determined with less precision than m_0 and since k^- and χ are mutually dependent in our data analysis. The values given in the literature for k^- generally refer to equilibrium and kinetic dissociation measurements for oxygen binding to the heme. Values for the rate of oxygen exit from the protein matrix of myoglobin are provided by flash-photolysis experiments (14). However, different values are presented in those studies ranging from 10^6 s^{-1} to 10^9 s^{-1}, which depend upon the model utilized. Comparison of our k^- with the literature is not, then, straightforward.

The ratio k^+/k^- can yield the average number of oxygens per protein; these values are reported in Table III for $Mb^{des\ Fe}$ and $Hb^{des\ Fe}$ in the presence and absence of sucrose. We note that the units of k^+ are $M^{-1}s^{-1}$ where M^{-1} refers to the concentration of oxygen in the solution. Because protein concentration was very low compared with oxygen concentration, the rate constant became pseudo-first order. Our k^+ term, then, accounts for the difference in the solution oxygen concentration in the presence and absence of sucrose. We note that although the k^+/k^- ratio appeared independent of the nature of the solvent, the k^- term had a large uncertainty that precluded a rigorous statement about these ratios. The general magnitude of these ratios, however, allowed us to evaluate the partition coefficient α for oxygen between equal volumes of protein and solvent; these coefficients, reported in Table III, (protein to solvent) range between 0.3 ($Mb^{des\ Fe}$) and 0.6 ($Hb^{des\ Fe}$). The ratio $k^+[Q]/k^-$ gave the average number of oxygen molecules per protein, and the partition coefficient was evaluated from solubility data on oxygen in water and sucrose solutions and from the protein volume that was taken as 44 liters · mol^{-1} and 12 liters · mol^{-1} for $Hb^{des\ Fe}$

and $Mb^{des\ Fe}$, respectively. The values obtained for the partition coefficient indicate that oxygen does not accumulate substantially in the protein interior, contrary to some points of view that hold that protein interiors are highly hydrophobic and readily accumulate oxygen. Knowledge of the partition coefficient does not reveal the details of the distribution. Certainly, regions of the protein exist (rigid domains for example) that would not accommodate significant amounts of oxygen, whereas other regions may be more hospitable.

We note that the oxygen concentration in the protein must be in equilibrium with the gas phase; addition of sucrose then should not perturb this equilibrium unless the protein characteristics are modified. Our observed changes in k^+ and k^- for $Mb^{des\ Fe}$ and $Hb^{des\ Fe}$ in the presence and absence of sucrose suggest that some dynamic mechanism responsible for the magnitude of these individual rates is solvent dependent. Whether the primary cause involves the effect of solvent viscosity on the protein dynamics (17–19), the hydration at the protein surface or some other aspect of the protein interior is not evident at this time.

The values obtained were used to calculate an apparent bimolecular quenching rate constant, k^*_{app}, in the protein interior, assuming free diffusion. To obtain k^*_{app} we divided χ by the apparent molarity of oxygen in the protein interior. This approach leads to rather large values for k^*_{app}, ranging from $\sim 10^9\ M^{-1}s^{-1}$ to $10^{10}\ M^{-1}s^{-1}$, as shown in Table III. These values compare well with the bimolecular quenching constant found for many globular proteins (2). If a smaller volume is accessible for free diffusion than the volume of the entire protein, then a lower k^*_{app} value would be obtained. Presumably some regions or domains of highly organized secondary structure can inhibit oxygen diffusion. If only one-tenth of the protein interior is accessible, then the calculated k^*_{app} in Table III will be a factor of 10 too large. This observation merits particular attention, since k^*_{app} is used to estimate the time scale for fluctuations of the protein structure that permit migration of oxygen inside the protein matrix. We also note that χ appears to be effected by solvent viscosity. Such an effect is predicted (18) on the basis of a theory for the coupling between the solvent and the protein dynamics and has been observed (19), but the uncertainties in our values preclude a rigorous comparison with theory at this point.

At present, we may only speculate on the microscopic origins of the rates k^+, k^-, and χ. Entry or exit of a small uncharged molecule from the protein interior may depend upon several mechanisms such as energy barriers at the protein surface due to the hydration shell, gate-like mechanisms including specific movements of amino-acid residues, or general fluctuations or dynamics of the protein structure. The microscopic details of the migration process in the protein interior that determine χ may be described by a discrete number of energy barriers, a discrete number of specific pathways, or a more general, random-walk type mechanism, the character of which may vary in different protein regions. Clearly, elucidation of these processes requires more experimental details including the effect of solvent modification, temperature, and quencher properties.

Up to this point, the discussion has concerned only data obtained in the low quencher concentration regime. In the high quencher concentration regime, the details of quencher distribution add a new aspect to the analysis (see preceeding article). At present, attempts to take these factors rigorously into account seem premature.

As shown in the preceeding article (10) the equations developed for the analysis of lifetime quenching data can be used to calculate the intensity quenching. In Figs. 10 and 11 we report the observed intensity quenching (solid lines) for $Hb^{des\ Fe}$ and $Mb^{des\ Fe}$ in the presence and absence of sucrose, as well as the calculated intensity quenching curves based on the use of Eq. 7 of the preceeding article. We note the deviation of the observed and calculated curves, which suggests that our initial treatment was not adequate. We also note that these deviations are generally smaller for $Hb^{des\ Fe}$ than for $Mb^{des\ Fe}$. As Keizer (20) has demonstrated, the details of the quencher distribution around a fluorophore in a homogeneous solvent can affect the observed intensity quenching. In the case of proteins, this distribution depends upon the details of the protein structure and dynamics. If a distribution favors the placement of some quenchers in close spatial or temporal proximity to the fluorophore, then the effective quenching rate for these proximate quenchers will be substantially larger than the average quenching rate. In the limit, such

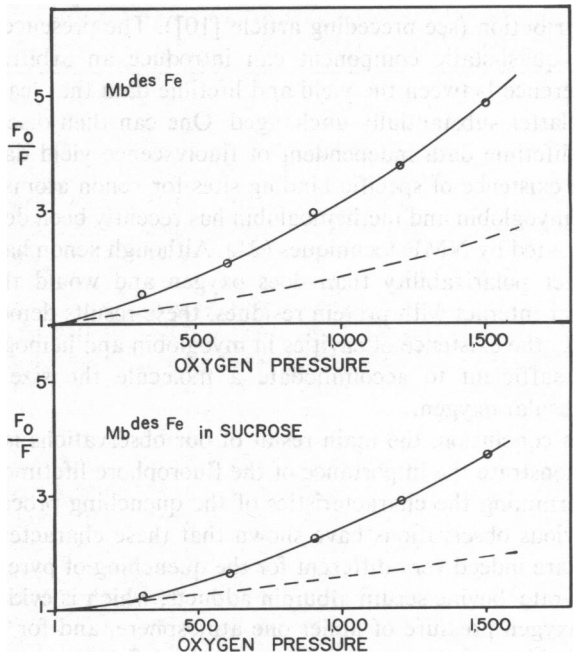

FIGURE 10 Intensity quenching of $Mb^{des\ Fe}$ in the absence (*top*) and presence (*bottom*) of 40% sucrose. Broken lines (---) correspond to the quenching curves calculated from the lifetime data as discussed in the text. Oxygen pressure given in pounds per square inch.

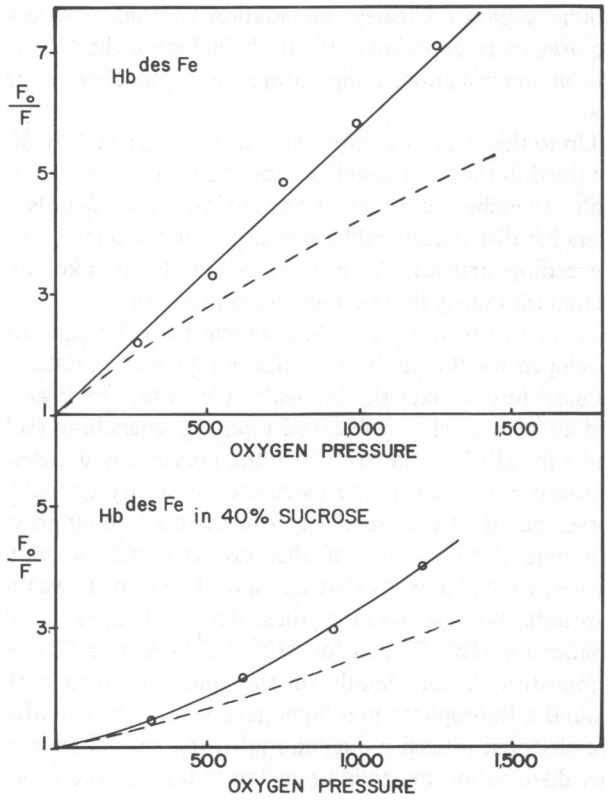

FIGURE 11 Intensity quenching of $Hb^{des\ Fe}$ in the absence (*top*) and presence (*bottom*) of 40% sucrose. Broken lines (---) correspond to the quenching curves calculated from the lifetime data as discussed in the text. Oxygen pressure given in pounds per square inch.

an effect amounts to the presence of a static quenching contribution (see preceding article [10]). The presence of this quasi-static component can introduce an arbitrary difference between the yield and lifetime data that leaves the latter substantially unchanged. One can then discuss the lifetime data independent of fluorescence yield data. The existence of specific binding sites for xenon atoms in metmyoglobin and methemoglobin has recently been demonstrated by NMR techniques (21). Although xenon has a higher polarizability than does oxygen and would thus better interact with protein residues, these results demonstrate the existence of cavities in myoglobin and hemoglobin sufficient to accommodate a molecule the size of molecular oxygen.

In conclusion, the main result of our observations is to demonstrate the importance of the fluorophore lifetime in determining the characteristics of the quenching process. Previous observations have shown that these characteristics are indeed very different for the quenching of pyrene-butyrate–bovine serum albumin adducts, which is evident at oxygen pressure of under one atmosphere, and for the quenching of the short-lived tryptophan fluorescence of many proteins, which requires tens of atmospheres of oxygen pressure. In the quenching of our porphyrin-proteins the intermediate aspects linking these two oxygen concentration regimes became apparent. We can follow the transition from one regime to another and observe the consequent increase in the complexity of the process. We now need to take cognizance of both the rate of penetration of oxygen in the protein interior and its further migration to the fluorophore. The former rate is the prime determinant of the quenching phenomena of the long lived pyrene fluorescence and the latter rate is dominant in the quenching of tryptophan fluorescence.

We would like to acknowledge the financial support of the National Science Foundation grant PCM 79-18646 and Biomedical Research Support grant PHS-2-507-RR07030-16 to Dr. Gratton, Institut National de la Santé et de la Recherche Medical and Centre National de la Recherche Scientifique to Dr. Alpert, and PHS-GM-11223 to Dr. Weber.

Received for publication 25 July 1983 and in final form 29 November 1983.

REFERENCES

1. Eftink, M. R., and C. A. Ghiron 1981. Fluorescence quenching studies with proteins. *Anal. Biochem.* 114:199–227.
2. Lakowicz, J. R., and G. Weber. 1973. Quenching of protein fluorescence by oxygen. Detection of structural fluctuations in proteins on the nanosecond time scale. *Biochemistry.* 12:4171–4179.
3. Handbook of Chemistry and Physics. 1974. CRC Press, Cleveland, OH. 55th ed. D-23.
4. Sebban, P., M. Coppey, B. Alpert, L. Lindqvist, and D. M. Jameson. 1980. Fluorescence properties of porphyrin-globin from human hemoglobin. *Photochem. Photobiol.* 32:727–731.
5. Lakowicz, J. R., and G. Weber. 1973. Quenching of fluorescence by oxygen. A probe for structural fluctuations in macromolecules. *Biochemistry.* 12:4161–4170.
6. International Critical Tables. 1928. E. W. Washburn, editor. First ed. McGraw-Hill, Inc., N.Y. 3:257, 272.
7. Coppey, M. 1981. Role de l'heme et de la proteine dans le measure d'oxygenation de l'hemoglobin. Ph.D thesis, Université de Paris VII, Paris, France.
8. Gratton, E., and M. Limkeman. 1984. A continuously variable frequency cross-correlation phase fluorometer with picosecond resolution. *Biophys. J.* 44:315–324.
9. Weber, G. 1981. Resolution of the fluorescence lifetimes in a heterogeneous system by phase and modulation measurements. *J. Phys. Chem.* 85:949–953.
10. Gratton, E., B. Alpert, D. M. Jameson, and G. Weber. 1984. Model of dynamic quenching of fluorescence in globular proteins. *Biophys. J.* 45:789–794.
11. Jameson, D. M., and E. Gratton. 1983. Analysis of heterogeneous emissions by phase and modulation fluorometry. *In* New Directions in Molecular Luminescence. D. Eastwood and L. Cline-Love, editors. American Society for Testing and Materials, Philadelphia, PA. 67–81.
12. Jameson, D. M., E. Gratton, and R. D. Hall. 1984. The measurement and analysis of heterogeneous emissions by multifrequency phase and modulation fluorometry. *Appl. Spectrosc. Rev.* 20:55–106.
13. Coppey, M., D. M. Jameson, and B. Alpert. 1981. Oxygen diffusion through hemoglobin and $Hb^{des\ Fe}$. *FEBS (Fed. Eur. Biochem. Soc.) Lett.* 126:191–194.
14. Austin, R. H., K. W. Beeson, L. Eisenstein, H. Frauenfelder, and I. C. Gunsalus. 1975. Dynamics of ligand binding to myoglobin. *Biochemistry.* 14:5355–5373.
15. Vaughan, W. M., and G. Weber. 1970. Oxygen quenching of

pyrenebutyric acid fluorescence in water. A dynamic probe of the microenvironment. *Biochemistry.* 9:466–473.

16. Alpert, B., and L. Lindqvist. 1975. Porphyrin triplet state probing the diffusion of oxygen in hemoglobin. *Science (Wash, DC).* 187:836–837.
17. Eftink, M. R., and C. A. Ghiron. 19 . Exposure of tryptophanyl residues and protein dynamics. *Biochemistry.* 16:5546–5551.
18. Doster, W. 1983. Viscosity scaling and protein dynamics. *Biophys. Chem.* 17:97–103.
19. Beece, D., L. Eisenstein, H. Frauenfelder, D. Good, M. C. Marden, L. Reinisch, A. H. Reynolds, L. B. Sorenson, and K. T. Yue. 1980. Solvent viscosity and protein dynamics. *Biochemistry.* 19:5147–5157.
20. Keizer, J. 1983. Nonlinear fluorescence quenching and the origin of positive curvature in Stern-Volmer plots. *J. Am. Chem. Soc.* 105:1494–1498.
21. Tilton, R. F., Jr., and I. D. Kuntz, Jr. 1982. Nuclear magnetic resonance studies of ^{129}Xe with myoglobin and hemoglobin. *Biochemistry.* 21:6850–6857.